Japanese Journal of Applied Physics
Vol. 44, No. 10, 2005, pp. 7309–7313
©2005 The Japan Society of Applied Physics

Host Isotope Effect on the Local Vibration Modes of VH_2 and VOH_2 Defects in Isotopically Enriched ^{28}Si, ^{29}Si and ^{30}Si Single Crystals

Takeru OHYA, Kohei M. ITOH, Rui N. PEREIRA[1] and Brian Bech NIELSEN[1]

Department of Applied Physics and CREST-JST, Keio University, Yokohama 223-8522, Japan
[1]*Department of Physics and Astronomy, University of Aarhus, DK-8000 Aarhus, Denmark*

(Received March 3, 2005; accepted July 25, 2005; published October 11, 2005)

Local vibrational modes of a vacancy with two hydrogen atoms (VH_2) and of a vacancy with one oxygen and two-hydrogen atoms (VOH_2) in silicon have been investigated using isotopically enriched ^{28}Si, ^{29}Si, and ^{30}Si single crystals. Infrared absorption spectroscopy revealed shifts in the Si–H stretch frequencies of the two defects when the mass of the silicon host atoms was changed. The observed stretch frequencies can for each defect be accounted for with a simple vibrational model based on two coupled Morse oscillators. The anharmonic contribution to the local vibrational mode frequencies of these two defects is evaluated. [DOI: 10.1143/JJAP.44.7309]

KEYWORDS: Silicon, oxygen, defect, local vibrational mode, isotope engineering, infrared spectroscopy

1. Introduction

Localized vibrations of impurity atoms in semiconductors occur when the mass of the impurity atoms is smaller than that of host atoms. Hydrogen as an impurity atom is an attractive choice for investigations of localized vibrational modes in semiconductors because 1) it is the lightest element in the periodic table, 2) it forms a large number of complexes with lattice defects and other impurity atoms, which ensures that enough information can be collected to achieve a detailed understanding of the vibrational problem, and 3) it can be introduced very easily by a variety of methods including exposure to H-plasma, annealing in a H_2 atmosphere, implantation of protons, and by various etching processes. In fact, introduction of hydrogen is almost unavoidable in processing of state-of-the-art integrated circuits based on silicon and optical devices based on compound semiconductors. Hence, an in-depth understanding of the properties of hydrogen, including its localized vibrational modes, may lead to improved device performance and to development of new characterization tools for hydrogen by semiconductor engineers.[1–5]

This paper describes the localized vibrational modes of a vacancy with two hydrogen atoms (VH_2) and of a vacancy with one oxygen and two-hydrogen atoms (VOH_2) in silicon. Hydrogen in silicon single crystals can exist as an isolated impurity atom, as H_2 molecules, and as a constituent of defect complexes, where the hydrogen atoms form bonds to host atoms, shallow impurities, transition metals, carbon, oxygen, etc.[1–4] The local structures of such defects have been determined using a variety of characterization tools such as deep level transient spectroscopy (DLTS), electron paramagnetic resonance (EPR), Fourier transform infrared spectroscopy (FTIR), and Raman spectroscopy. The local vibrational modes may be detected by FTIR and Raman spectroscopy. When these techniques are employed, the involvement of hydrogen is confirmed by observation of the large frequency shift when hydrogen is substituted by deuterium. The ratio between the mode frequencies for hydrogen and deuterium is close to $\sqrt{2}$. In many hydrogen-related complexes, the hydrogen atom forms a covalent bond with a host atom. In such cases, the neighboring host atom will participate weakly in the local mode oscillation and therefore, a small frequency shift will result if the isotope of the host atom is changed. However, the isotopic composition of naturally available silicon is always fixed at 92.2% ^{28}Si, 4.7% ^{29}Si, and 3.1% ^{30}Si, and the absorption due to Si–H stretch and bend modes associated with ^{29}Si–H and ^{30}Si–H bonds are normally masked by the much stronger absorption from ^{28}Si–H bonds. In order to overcome this limitation, we have recently succeeded in producing nearly monoisotopic crystals of the three stable isotopes ^{28}Si, ^{29}Si, and ^{30}Si, and thereby added a new degree of freedom to localized vibrational mode studies in silicon.[6,7] We took advantage of this and investigated the effect of host silicon isotopes on localized vibrational modes of oxygen[8] and hydrogen.[9] Among the new findings reported in these studies, the most notable results are found for positively charged bond-center hydrogen (H_{BC}^+), which is one of the most extensively studied hydrogen defects.[10–12] When the mass of host silicon atoms is increased from ^{28}Si to ^{30}Si, the mode frequency changes in opposite directions for bond-center hydrogen and bond-center deuterium.[9] These results could be satisfactorily modeled only when anharmonic terms are included in the vibrational potential.[9] It is of great interest to extend such studies to other hydrogen-related defects in silicon where the bonding configurations and charge states are different from H_{BC}^+. Such complexes can be readily introduced into silicon by proton implantation or by electron irradiation of silicon containing hydrogen. Vacancies and interstitials are produced by proton implantation as well as electron irradiation. Both type of defects possess dangling bonds which represent strong trap sites for hydrogen. As a result, a large number of vacancy-hydrogen and interstitial-hydrogen defects are formed. The local vibrational modes of these defects have been studied extensively by FTIR spectroscopy. The frequency shifts when hydrogen is substituted by deuterium has been established for a number of these defects and valuable information about the number of hydrogen atoms involved in the defects has been obtained from samples co-doped with hydrogen and deuterium.[13–19] The present study focuses on the frequency shifts that result when the silicon isotope is changed. We shall refer to these shifts as silicon isotope shifts and we will focus on the vacancy containing two hydrogen atoms (VH_2)[13,14] and on the vacancy containing two hydrogen and one oxygen atom (VOH_2).[16,18,19] The structure proposed for VH_2 is shown in Fig. 1, where the open circles denote silicon atoms and the

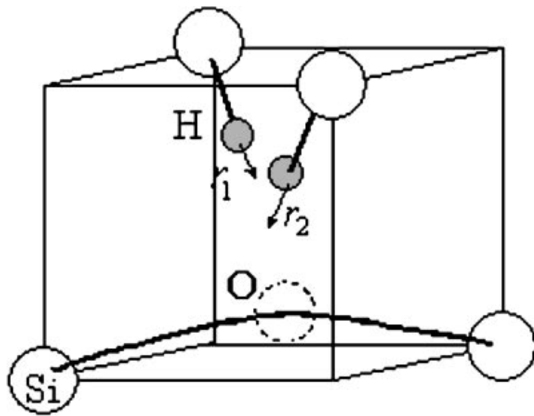

Fig. 1. Structures of VH_2 and VOH_2 defects. VH_2 involves no oxygen while one oxygen atom is placed at the position of dashed-circle in the case of VOH_2 defect. r_1 and r_2 are the displacement vectors of the respective Si–H bonds.

gray circles represent hydrogen atoms. Note that the vacancy is located at the center of the cube. For the VOH_2 complex, the positions of the silicon and the hydrogen atoms and the vacancy remain approximately the same as for VH_2 but one oxygen atom is inserted at the position denoted by the dashed circle. The present study deals only with the stretch modes where the hydrogen atoms oscillate along the displacement vectors r_1 and r_2, which define bond extensions at a given time. There are two stretch modes, one with A_1 in which a pair of H atoms oscillates symmetrically and one with the B_1 symmetry in which a pair of H atoms oscillates asymmetrically.

2. Experiments

Samples were Czochralski-grown Si single crystals that were isotopically enriched with either ^{28}Si, ^{29}Si or ^{30}Si. The samples applied in the study of VH_2 were enriched to ^{28}Si (99.93%), ^{29}Si (97.10%), and ^{30}Si (99.75%), and the samples applied in the investigation of VOH_2 were enriched to ^{28}Si (99.85%), ^{29}Si (99.23%), and ^{30}Si (99.75%) with the oxygen concentration $\sim 10^{18}$ cm^{-3}. The growth and the characterization of the as-grown crystals, i.e., before introduction of hydrogen defects, have been described in ref. 6 to which the interested reader is referred.

The implantation of H and D and the subsequent absorption measurements to investigate VH_2 were performed at the University of Aarhus. Each sample was placed in a cryostat equipped with two CsI windows for optical measurements and an 0.2 mm thick Al window. The cryostat was mounted inside a vacuum chamber connected to a tandem accelerator. Protons or deuterons were implanted with different energies in the range 5–10 MeV through the aluminum window into the sample. The energy and dose at each implantation step were carefully set to result in homogeneous hydrogen concentration of 10^{18}–10^{19} cm^{-3} in the region from 150 to 550 μm below the implanted surface. The temperature on the sample was monitored during the implantation and always kept below 20 K. Immediately after the implantation, the cryostat was transferred to the infrared spectrometer without raising the sample temperature above 20 K. Subsequently an isochronal annealing sequence was performed. In each step the sample was given a 30-min anneal at a predetermined temperature and then cooled to 8 K, where an FTIR spectrum was recorded. The annealing temperature increased in each step with the first step at 120 K and the last step at 280 K. The infrared absorption measurements were carried out with a Nicolet, System 800 FTIR spectrometer, equipped with a globar light source, a Ge–KBr beam splitter, and a mercury cadmium telluride detector. The spectra were recorded at 8 K with an apodized resolution of 0.25 cm^{-1}.

The samples for investigation of VOH_2 was prepared and measured at Keio University. The samples were sealed in quartz capsules together with H_2 and D_2 gas. The capsules were annealed at 1300°C for an hour followed by quenching into water. At this point, H and D atoms should be distributed uniformly throughout the samples in the form of H_2, D_2 and HD molecules.[20] In order to introduce irradiation defects, the samples were then irradiated with 3 MeV electrons at room temperature with an irradiation dose of 1×10^{17} cm^{-2}. To avoid unintentional annealing, the samples were pressed onto sample holder that was cooled with water. Every sample was irradiated with the same dose on both sides to ensure uniform damage distribution throughout the 6-mm-thick samples. The infrared absorption measurements were performed with a BOMEM DA8 FTIR spectrometer, equipped with a glowbar light source, KBr beam splitter, and a mercury-cadmium-telluride detector. The spectra were recorded at $\sim$8 K with an apodized resolution 0.25 cm^{-1}.

3. Results and Discussions

Figure 2 shows the infrared absorption spectra recorded on the ^{28}Si-, ^{29}Si-, and ^{30}Si-enriched crystals after proton implantation. The asymmetric B_1 modes of VH_2 is clearly resolved, whereas the symmetric A_1 mode is weak and barely resolved. As can be seen from the figure the frequencies shift downwards by about 2 cm^{-1}, when the silicon mass is increased from 28 amu to 30 amu. This is in agreement with common wisdom that the frequency should decrease when the mass of the oscillator increases.

In Fig. 3 the infrared absorption spectra recorded on the $H_2 + D_2$-annealed and electron irradiated-^{29}Si- and ^{30}Si-enriched samples. The absorption lines denoted A_1 and B_1 represent the symmetric and the asymmetric stretch modes of VOH_2,[18] whereas the line denoted A' represents the Si–H stretch mode of VOHD.[18] These modes are clearly resolved in the spectrum recorded on the ^{30}Si-enriched sample, whereas only the B_1 and the A' modes are (barely) resolved in the ^{29}Si-enriched sample. Unfortunately, the stretch modes associated with VOH_2 were not observed in the ^{28}Si-enriched sample, probably due to a low oxygen concentration in this sample. We note that the silicon mass isotope shift of the mode frequencies is qualitatively similar to that for VH_2, i.e., a downward shift when the silicon is increased.

In our previous study on the local mode of H_{BC}^+,[9] we observed that the silicon isotope shifts were in opposite directions for H_{BC}^+ and D_{BC}^+. As mentioned above we succeeded to explain these results with a model including anhamonicity. A similar model based on the anharmonic Morse potential, which was used successfully for the modeling of VH_2 in natural Si,[13] is employed in this study

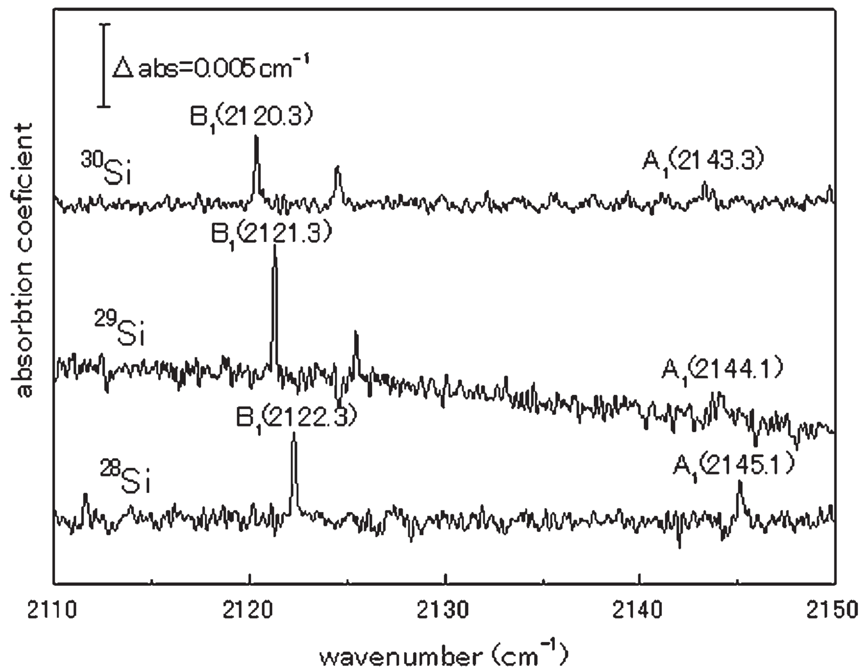

Fig. 2. Absorption spectra of proton-implanted ^{28}Si, ^{29}Si and ^{30}Si. Wavenumber labeled peaks are due to localized vibrational modes of VH_2.

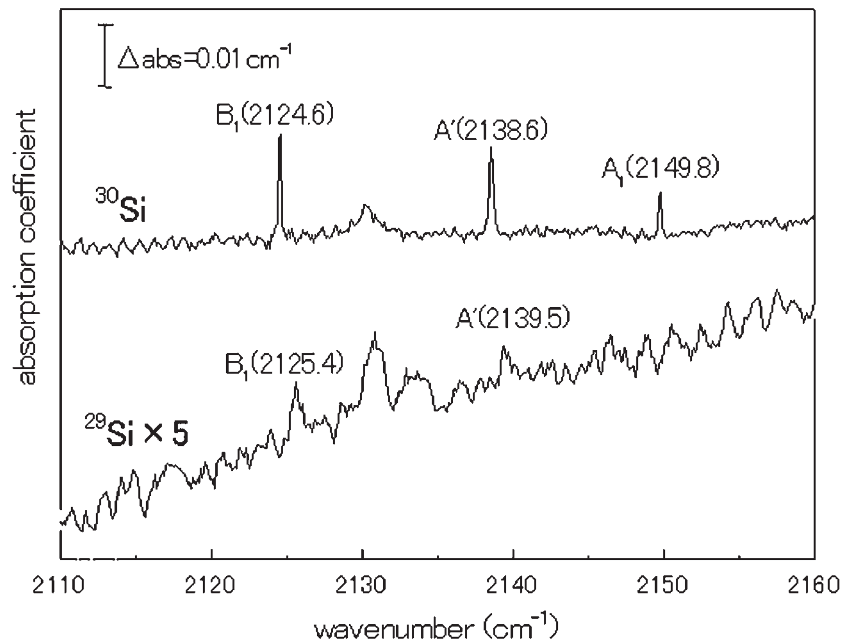

Fig. 3. Fragments of the absorption spectra of H_2-annealed ^{29}Si and ^{30}Si. Peaks applied position are due to LVMs of V–O–H_2. Corresponding peaks are not observed in our ^{28}Si sample due to the lack of oxygen concentration.

to evaluate the silicon isotope effect on the local vibrational modes of VH_2 and VOH_2. Using the Morse potential as a model potential for the stretching of each bond the Hamiltonian for the system may be expressed as;

$$H = -\frac{\hbar^2}{2\mu_1}\frac{\partial^2}{\partial {r_1}^2} - \frac{\hbar^2}{2\mu_2}\frac{\partial^2}{\partial {r_2}^2} + D_1(1 - e^{-\alpha_1 r_1})^2 + D_2(1 - e^{-\alpha_2 r_2})^2 + f_{12} r_1 r_2 + f_{112}({r_1}^2 r_2 + r_1 {r_2}^2) \quad (1)$$

where r_1 and r_2 are the displacement coordinates shown in Fig. 1, D_i and α_i are the constants for the two hydrogen labeled by $i = 1$, 2, and f_{12} and f_{112} are harmonic and anharmonic coupling constants between the two bonds, respectively.[16] Noting the symmetry of the defect, we set $D = D_1 = D_2$ and $\alpha = \alpha_1 = \alpha_2$. D is the depth of the potential while $1/\alpha$ is a measure of the width (or curvature) of the potential. Finally, μ_i is the effective mass, which we in accordance with normal practice assume for two point-masses connected to each other, may be expressed as;

$$\frac{1}{\mu_i} = \frac{1}{m_{\mathrm{H\ or\ D}}} + \frac{1}{\chi m_{\mathrm{Si}}} \quad (2)$$

where χ is a factor that gives a measure of the effective mass

of the silicon atom bonded to the H (D) atom.[21] The vibrational frequencies calculated with our model do not depend critically on χ since the mass of hydrogen (m_H) and deuterium (m_D) is much smaller than the mass of silicon (m_{Si}). Hence, we set $\chi = 1$ in our calculation, which is the value for a silicon with no neighboring atoms. The coupling terms are expected to be much smaller than the Morse potential-terms and may therefore e treated as perturbations. Furthermore, we may simplify the problem by expanding the Morse potential terms to fourth order;

$$H = -\frac{\hbar^2}{2\mu_1}\frac{\partial^2}{\partial {r_1}^2} - \frac{\hbar^2}{2\mu_2}\frac{\partial^2}{\partial {r_2}^2} + \frac{1}{2}f({r_1}^2 + {r_2}^2) + f_3({r_1}^3 + {r_2}^3) + f_4({r_1}^4 + {r_2}^4) + f_{12}r_1r_2 + f_{112}({r_1}^2 r_2 + r_1{r_2}^2) \quad (3)$$

where

$$f = 2D\alpha^2, \quad f_3 = -D\alpha^3, \quad f_4 = \frac{7}{12}D\alpha^4. \quad (4)$$

As a result, the vibrational problem can be treated by perturbation theory where the unperturbed Hamiltonian consists of the first three terms on the right hand side of eq. (3). Hence our unperturbed eigenfunctions are those of two identical and uncoupled harmonic oscillators, for which the relevant matrix elements may be found in standard tables. For the harmonic coupling term $f_{12}r_1r_2$ and the quartic terms we calculate the first-order correction to the energy of the vibrational ground state and the first excited state, whereas the second-order correction is calculated for the cubic terms since they do not contribute to first order. Alternatively, the harmonic coupling term $f_{12}r_1r_2$ might have been included in the unperturbed Hamiltonian but as long as $f_{12}/f \ll 1$, the first order correction gives an accurate estimate.

The parameters D, α, f_{12} and f_{112} in eq. (3) will depend weakly on the mass of the silicon isotope because the lattice constant of isotopically enriched ^{28}Si, ^{29}Si and ^{30}Si are slightly different due to anharmonic effect. However, we shall assume that the effect on the mode frequencies may be neglected, and thus, it is possible to calculate frequencies of the stretch modes for VH_2, VD_2 and VHD in the ^{28}Si, ^{29}Si and ^{30}Si samples using a single set of parameters D, α, f_{12} and f_{112}. We have adjusted these parameters to obtain the best fit and the results shown in Table I are in excellent agreement with the experimentally observed mode frequencies.

The *ab initio* calculation by Markevich *et al.* indicates that the hydrogen vibrations are dynamically decoupled from the vibrations of the oxygen atom in the VOH_2 defect.[17] We may therefore ignore the presence of the O atom and analyze VOH_2 in the same manner as VH_2 using eq. (3). The presence of oxygen atom will of course modify the force constant somewhat and this will be reflected in the values of D, α, f_{12} and f_{112} obtained from the fit to the experimental data. The results obtained from the fit are shown in Table II. As expected, the values of D, α, f_{12} and f_{112} are changed, but only slightly, compared to the values for VH_2 shown in Table I. Again the agreement between experimental and calculated frequencies is very good.

The anharmonic contribution ω_{anharm} of H_{BC}^+ (~ -150 cm^{-1}) is $\sim$7% of the harmonicnic term ω_{harm}[9] and thus relatively larger than those for VH_2 and VOH_2 (~ -110 cm^{-1}), which are $\sim$5% of ω_{harm}. For the difference between VH_2 and VOH_2, our results show a slightly shallower (D for VH_2 is smaller than D for VOH_2) and narrower (α for VH_2 is larger than α for VOH_2) potential well for VH_2 than for VOH_2. This narrower potential well for VH_2 leads to the larger anharmonicity observed for the modes of this defect. Most of the previous theoretical studies successfully predicted the structures of VH_2 and VOH_2 and gave values for the Si–H and H–H equilibrium distances.[18,22–24] We have determined the vibrational potentials of these defects in the present study and it will be of great interest to compare the theoretical potentials with those presented in this work. However, further theoretical work is needed before such a comparison can be made.

Table I. Comparison of the model calculations ω_{model}, which is composed of the harmonic and anharmonic terms ($\omega_{model} = \omega_{harm} + \omega_{anharm}$), with the experimental results ω_{obs} for VH_2 in the unit of cm^{-1}. An approximate error bar on ω_{obs} is ± 0.03 cm^{-1}. Experimental values of VD_2 and VHD in ^{28}Si are taken from H_2 and D_2 annealed sample, i.e., the corresponding peaks are not present in Fig. 1. The values of the parameters employed as a result of fitting are $D = 2.9760$ eV, $\alpha = 1.7324$ Å^{-1}, $f_{12} = 0.28914$ eV/Å^2, and $f_{112} = -0.78858$ eV/Å^3.

Host	Defects	Mode	ω_{harm}	ω_{anharm}	ω_{model}	ω_{obs}	$\omega_{obs} - \omega_{model}$
^{28}Si	VH_2	A_1	2261.0	−115.7	2145.3	2145.1	−0.2
		B_1	2224.7	−102.1	2122.6	2122.3	−0.3
	VD_2	B_1	1600.0	−52.8	1547.2	1547.8	0.6
	VHD	A′	2242.9	−107.8	2135.1	2135.4	0.3
		A′	1613.1	−57.1	1535.9	1555.3	−0.6
^{29}Si	VH_2	A_1	2259.7	−115.6	2144.1	2144.1	0.0
		B_1	2223.4	−102.0	2121.4	2121.3	−0.1
^{30}Si	VH_2	A_1	2258.4	−115.4	2143.0	2143.3	0.3
		B_1	2222.2	−101.9	2120.3	2120.3	0.0

Table II. Comparison of the model calculations ω_{model}, which is composed of the harmonic and anharmonic terms ($\omega_{model} = \omega_{harm} + \omega_{anharm}$), with the experimental results ω_{obs} for VOH_2 in the unit of cm^{-1}. An approximate error bar for ω_{obs} is ± 0.03 cm^{-1}. Some of the experimental values have been taken from ref. 9 as indicated. The values of the parameters employed as a result of fitting are $D = 3.3204$ eV, $\alpha = 1.6347$ Å^{-1}, $f_{12} = 0.26823$ eV/Å^2, and $f_{112} = -0.54672$ eV/Å^3.

Host	Defects	Mode	ω_{harm}	ω_{anharm}	ω_{model}	ω_{obs}	$\omega_{obs} - \omega_{model}$
^{28}Si	VOH_2	A_1	2252.4	−100.5	2152.0	2151.5[9]	−0.5
		B_1	2218.6	−91.5	2127.1	2126.4[9]	−0.7
	VOD_2	A_1	1619.9	−52.0	1568.0	1567.4[9]	−0.6
		B_1	1595.6	−47.4	1548.3	1549.1[9]	0.8
	VOHD	A′	2235.5	−95.3	2140.5	2140.6[9]	0.1
		A′	1607.8	−50.2	1557.6	1557.3[9]	−0.3
^{29}Si	VOH_2	B_1	2217.3	−91.4	2125.9	2125.4	−0.5
	VOHD	A′	2234.2	−95.1	2139.1	2139.5	0.4
^{30}Si	VOH_2	A_1	2249.8	−100.2	2149.6	2149.8	0.2
		B_1	2216.1	−91.3	2124.7	2124.6	−0.1
	VOHD	A′	2232.9	−95.0	2137.9	2138.6	0.7

4. Conclusion

In this work, frequencies of LVMs related to VH_2 and V–O–H_2 in ^{29}Si and ^{30}Si were identified. Host-isotope shifts

observed in these two defects were well reproduced by a simple vibrational model based on two-coupled Morse oscillators.

Acknowledgement

The authors wish to thank the Professor M. Suezawa of Tohoku University for fruitful discussion and H. Hanaya of the JAERI Takasaki Institute for his help in electron irradiation.

1) *Hydrogen in Semiconductors*, eds. J. I. Pankove and N. M. Johnson (Academic, New York, 1990) Semiconductors and Semimetals, Vol. 34.
2) S. J. Pearton, J. W. Corbett and M. Stavola: *Hydrogen in Crystalline Semiconductors* (Springer-Verlag, Berlin, 1992).
3) S. K. Estreicher: Mater. Sci. Eng. Rep. **14** (1995) 319.
4) *Hydrogen in Semiconductors II*, ed. N. H. Nickel (Academic, New York, 1999) Semiconductors and Semimetals, Vol. 61.
5) J. W. Lyding, K. Hess and I. C. Kizilyalli: Appl. Phys. Lett. **68** (1996) 2526.
6) K. Takyu, K. M. Itoh, K. Oka, N. Saito and V. I. Ozhogin: Jpn. J. Appl. Phys. **38** (1999) L1493.
7) K. M. Itoh, J. Kato, F. Uemura, A. K. Kaliteyevskii, O. N. Godisov, G. G. Devyatych, A. D. Bulanov, A. V. Gusev, I. D. Kovalev, P. G. Sennikov, H.-J. Pohl, N. V. Abrosimov and H. Riemann: Jpn. J. Appl. Phys. **42** (2003) 6248.
8) J. Kato, K. M. Itoh, H. Yamda-Kaneta and H.-J. Pohl: Phys. Rev. B **68** (2003) 035205.
9) R. N. Pereira, T. Ohya, K. M. Itoh and B. Bech Nielsen: Physica B **340–342** (2003) 697.
10) H. J. Stein: Phys. Rev. Lett. **43** (1979) 1030.
11) K. Bonde Nielsen, B. Bech Nielsen, J. Hansen, E. Andersen and J. U. Andersen: Phys. Rev. B **60** (1999) 1716.
12) M. Budde, C. Parks Cheney, G. Lüpke, N. H. Tolk and L. C. Feldman: Phys. Rev. B **63** (2001) 195203.
13) B. Bech Nielsen, L. Hoffmann and M. Budde: Mater. Sci. Eng. B **36** (1996) 259.
14) E. V. Lavrov, J. Weber, L. Hung and B. Bech Nielsen: Phys. Rev. B **64** (2001) 035204.
15) M. Budde, B. Bech Nielsen, P. Leary, J. Goss, R. Jones, P. R. Briddon, S. Öberg and S. J. Breuer: Phys. Rev. B **57** (1998) 4397.
16) B. N. Mukashev, S. Z. Tokmoldin, M. F. Tamendarov and V. V. Frolov: Physica B **170** (1991) 545.
17) M. Suezawa: Phys. Rev. B **63** (2000) 035201.
18) V. P. Markevich, L. I. Murin, M. Suezawa, J. L. Lindström, J. Coutinho, R. Jones, P. R. Briddon and S. Öberg: Phys. Rev. B **61** (2000) 12964.
19) A. Nakanishi, N. Fukata and M. Suezawa: Physica B **308–310** (2001) 216.
20) R. E. Pritchard, M. J. Ashwin, J. H. Tucker, R. C. Newman, E. C. Lightowlers, M. J. Binns, S. A. McQuaid and R. Flaster: Phys. Rev. B **56** (1997) 13118.
21) R. C. Newman: Physica B **170** (1991) 409.
22) H. Xu: Phys. Rev. B **46** (1992) 1043.
23) M. A. Roberson and S. K. Estreicher: Phys. Rev. B **49** (1994) 17040.
24) B. Bech Nielsen, L. Hoffman, M. Budde, R. Jones, J. Gross and S. Öberg: Mater. Sci. Forum **196–201** (1995) 933.